Published as: *Cell Metab*. 2013 July 2; 18(1): 106–117.

Reciprocal Regulation of Hepatic and Adipose Lipogenesis by Liver X Receptors in Obesity and Insulin Resistance

Simon W. Beaven[1,2], **Aleksey Matveyenko**[3,4], **Kevin Wroblewski**[1], **Lily Chao**[1], **Damien Wilpitz**[1], **Tu Wen Hsu**[3,4], **Jacob Lentz**[2], **Brian Drew**[3], **Andrea L. Hevener**[3], and **Peter Tontonoz**[1]

[1]Howard Hughes Medical Institute, David Geffen School of Medicine at UCLA, Los Angeles, California, USA

[2]Division of Digestive Diseases, Department of Medicine, David Geffen School of Medicine at UCLA, Los Angeles, California, USA

[3]Division of Endocrinology, Diabetes, and Hypertension, Department of Medicine, David Geffen School of Medicine at UCLA, Los Angeles, California, USA

[4]Larry Hillblom Islet Research Center, David Geffen School of Medicine at UCLA, Los Angeles, California, USA

SUMMARY

Liver X receptors (LXRs) regulate lipogenesis and inflammation, but their contribution to the metabolic syndrome is unclear. We show that LXR signaling is required for key aspects of the metabolic syndrome in obese mice. LXRαβ-deficient-*ob/ob* (LOKO) mice remain obese, but show reduced hepatic steatosis and improved insulin sensitivity compared to *ob/ob* mice. Impaired hepatic lipogenesis in LOKO mice is accompanied by reciprocal increases in adipose lipid storage, reflecting tissue-selective effects of LXR on the SREBP, PPARγ, and ChREBP lipogenic pathways. LXRs are essential for obesity-driven SREBP-1c and ChREBP activity in liver, but not fat. Furthermore, loss of LXRs in obesity promotes adipose PPARγ and ChREBP-β activity, leading to improved insulin sensitivity. LOKO mice also exhibit defects in beta-cell mass and proliferation despite improved insulin sensitivity. Our data suggest that sterol sensing by LXRs in obesity is critically linked with lipid and glucose homeostasis and provide insight into complex relationships between LXR and insulin signaling.

Keywords

Nuclear receptor; liver X receptor (LXR); peroxisome proliferator-activated receptor (PPAR); carbohydrate response element binding protein (ChREBP); insulin resistance; diabetes; obesity; metabolic syndrome; hepatic steatosis; insulin signaling

Correspondence: Peter Tontonoz, Howard Hughes Medical Institute, David Geffen School of Medicine at UCLA, 675 Charles E. Young Drive, South, MacDonald Research Labs 6-770, Los Angeles, California 90095, USA. Phone: (310) 206-4546; Fax: (310) 267-0382; ptontonoz@mednet.ucla.edu.

Disclosures: The authors declare that no conflict of interest exists and have no other disclosures to make.

INTRODUCTION

The metabolic syndrome is a constellation of interrelated disorders including obesity, insulin resistance / diabetes, dyslipidemia, fatty liver, hypertension, and atherosclerosis. The pathogenesis of this syndrome is multi-factorial but lipid, glucose, and inflammatory dysfunction—manifested as obesity and insulin resistance—appear to be central features (Olefsky and Glass, 2010). Excessive hepatic lipogenesis is a hallmark feature of many models of obesity and diabetes, although the causal relationship between tissue lipid accumulation and insulin resistance is unclear (Farese et al., 2012).

Liver X receptors (LXRs) are oxysterol-activated nuclear receptors with important roles in lipid and glucose management. They direct cholesterol uptake, transport, and excretion through the coordinate and tissue-selective regulation of their target genes (Peet et al., 1998; Repa et al., 2000a; Tontonoz and Mangelsdorf, 2003; Zelcer et al., 2009). LXRs are also central regulators of SREBP-1c expression and *de novo* lipogenesis (Repa et al., 2000a; Repa et al., 2000b; Schultz et al., 2000). LXRs integrate lipid and inflammatory signaling pathways in both the innate and adaptive immune systems (Bensinger et al., 2008; Hong et al., 2012; Joseph et al., 2004; Joseph et al., 2003; N et al., 2009; Zelcer and Tontonoz, 2006). Ligand activation of LXRs promotes cholesterol excretion (Peet et al., 1998; Schultz et al., 2000; Tontonoz and Mangelsdorf, 2003) and reduces inflammation, but simultaneously stimulates *de novo* lipogenesis of triglycerides (Repa et al., 2000a; Repa et al., 2000b; Schultz et al., 2000), a potentially deleterious effect contributing to hepatic steatosis and possibly hepatic insulin resistance (Grefhorst and Parks, 2009).

Although LXRs are known to modulate many metabolic and inflammatory pathways that could potentially influence the development of diabetes and insulin resistance, the contribution of LXR signaling to the pathogenesis of the metabolic syndrome is still unclear. Ligand activation of LXRs in the setting of diet-induced or genetic obesity improves whole body glucose disposal, both by improving peripheral glucose disposal into fat via upregulation of the glucose transporter, GLUT4, and by indirectly suppressing hepatic gluconeogenesis (Commerford et al., 2007; Grefhorst et al., 2005; Laffitte et al., 2003). But the *in vivo* contribution of LXR-dependent gene expression in the setting of obesity and diabetes remains to be established. A major obstacle to investigating these potential connections is the fact that LXR null mice are resistant to certain protocols of diet-induced obesity (Kalaany et al., 2005) and lose adipose tissue mass with age and cholesterol accumulation (Bradley 2007). Thus, it has been difficult to examine the role of LXR signaling in a syndrome that has obesity as a hallmark.

Previous work has shown that the LXR target gene, stearoyl Co-A desaturase 1 (*Scd1*), is an important determinant of obesity in leptin deficient mice (Cohen et al., 2002). More recently, suppression of the SREBP pathway in *ob/ob* mice by inactivating SCAP was reported to rescue hepatic steatosis, without affecting insulin resistance (Moon et al., 2012). Since LXRs are master transcriptional regulators of both SCD1 and SREBP-1c, we expected that deletion of LXRs in the *ob/ob* mouse would affect multiple aspects of the metabolic syndrome, and might phenocopy SCD1 deficiency. Surprisingly, we show here that mice deficient in both LXRα and LXRβ, when bred onto the *ob/ob* background (LOKO mice), are

not protected from obesity. However, they are completely protected from hepatic steatosis and show dramatic improvement in insulin sensitivity. LOKO mice trade reduced hepatic steatosis for increased adipose tissue mass and increased PPARγ signaling in fat. Paradoxically, LOKO mice are glucose intolerant and insulinopenic due to impaired pancreatic responsiveness to a glucose challenge. Collectively, our data provide insight into the complex relationships between sterol sensing, LXRs, and insulin signaling pathways in obesity.

RESULTS

LOKO mice are obese but protected from hepatic steatosis

To determine the consequences of LXR deletion in obesity, we analyzed wild-type (WT), *Lxr*αβ−/− (DKO), *ob/ob* (OB), and *ob/ob Lxr*αβ−/− (LOKO) mice. Given the difficulty in generating these compound mutant animals—both OB mice and LXRβ null mice are sterile and must be bred as heterozygotes—we chose to focus our analysis primarily on male LOKO mice. All mice in this study were bred onto a C57BL/6 background, backcrossed 10+ generations. There were no differences in food consumption across three months of measurements (data not shown). Total body weight was similar between OB and LOKO mice up to 24 weeks of age (Fig. 1A,B). However, internal organ sizes were markedly different for both liver and fat (Fig. 1C). LOKO livers were not steatotic and their normalized weights were reduced compared to OB mice. Conversely, the epididymal fat pads were reciprocally increased in size and total body adiposity was increased in LOKO mice.

We determined nutrient utilization by housing mice in metabolic chambers for 72 h and calculating the respiratory quotient. LOKO mice showed a trend toward carbohydrate oxidation as indicated by a higher RER of 0.935 vs. 0.903 (Fig. 1D and Fig. S1A). There was no difference in food consumption, but LOKO mice drank significantly more water during these experiments (Fig. S1B). Correspondingly, LOKO mice showed increased movement in the vertical axis, which would be required for increased access to the water dispenser (Fig. S1C). Fast protein liquid chromatography (FPLC) was used to determine the serum cholesterol and lipid profiles of the animals. LOKO mice have increased plasma cholesterol and diminished circulating triglycerides compared to OB mice (Figs. 1E and S1D). Plasma free fatty acids were also not different between the genotypes (Fig. S1E). This observation is consistent with established roles for LXRs in governing cholesterol transport and excretion as well as hepatic lipogenesis (Bradley et al., 2007; Peet et al., 1998; Schultz et al., 2000).

As the gross liver weights were reduced in LOKO mice we analyzed lipid content and inflammation in more detail. At 24 weeks of age aspartate aminotransferase (AST) and alanine aminotransferase (ALT), serum markers of hepatocellular damage and necroinflammatory activity, tended to be elevated in plasma of LXR DKO compared to WT mice (Fig. 2A), consistent with the known hyper-inflammatory state of these animals (Beaven and Tontonoz, 2006). OB mice showed a marked increase in both AST and ALT, but LOKO mice were partially protected, suggesting reduced hepatic inflammation. Analysis of inflammatory gene expression showed a trend towards reduced expression of

MCP-1 and CD68 (Fig. S2A), but the overall level of inflammatory transcript expression was low in both groups, consistent with the mildly elevated AST and ALT values. These results correlated with an almost complete absence of steatosis in LOKO liver, both grossly (Fig. 2B) and histologically (Fig. 2C). Although hepatic triglyceride content was markedly reduced in LOKO livers, an increase in hepatic cholesterol content was observed despite consumption of a regular chow diet (Fig. 2D). Both of these findings are consistent with the plasma cholesterol and triglycerides levels. Together, these data establish that an intact LXR pathway is required for the development of hepatic steatosis in OB mice.

To determine the molecular basis for the changes in hepatic lipid accumulation, we analyzed gene expression by real-time PCR. LOKO livers showed a marked reduction in the expression of genes related to hepatic lipogenesis, especially *Srebp1c*, *Scd1*, *Fas*, *Gk* and *Elovl6* (Fig. 2E). By contrast the expression of SREBP-2 and its downstream target genes were largely preserved (Fig. S2B). Genes involved in the oxidation of fatty acids (*Ucp2*, *Pparα*) were not significantly altered, while enzymes related to thyroid hormone action (*Dio2*, *Dio3)* were diminished (Fig. 2E and data not shown). We observed upregulation of *Pepck* and *Foxo1*, two genes with well-recognized roles in hepatic gluconeogenesis, consistent with LXR's known function in suppressing gluconeogenesis (Commerford et al., 2007; Laffitte et al., 2003). The expression of insulin receptor substrate 2 (*Irs*2) was also increased in LOKO livers, consistent with heightened insulin sensitivity. The expression of insulin receptor, insulin receptor substrate 1, and glucose-6-phosphatase was unaffected by genetic loss of LXRs. Overall, the pattern of gene expression in the liver revealed a marked reduction in the lipogenic program.

Loss of LXRs impairs beta-cell expansion in response to obesity

Given recent data suggesting that hepatic lipid accumulation is not always accompanied by insulin resistance (Minehira et al., 2008; Monetti et al., 2007; Moon et al., 2012), we investigated the consequence of LXR inactivation and amelioration of hepatic steatosis on systemic glucose metabolism in obesity. There was a trend toward fasting hyperglycemia and lower insulin in LOKO mice after a 12 h fast (Fig. 3A). During random sampling of non-fasting blood glucose concentrations we observed marked hyperglycemia in LOKO mice (Fig. 3B). This was accompanied by glycosuria assessed by urinalysis. In contrast, glucose was undetectable in urine collected from OB and lean (WT or LXR DKO) mice (Fig. 3B and data not shown). Since the glucocorticoid axis can affect circulating blood glucose, and LXR deficiency has been reported to impact corticosterone production (Cummins et al., 2006), we measured corticosterone levels in LOKO and OB mice and found no differences (Fig. S2C,D).

We next performed intraperitoneal glucose tolerance tests (GTTs). LOKO mice showed impaired glucose tolerance and the blood glucose excursion over time was elevated even compared to insulin resistant OB mice (Fig. 3C). Unexpectedly, this glucose intolerance correlated with a defect in second phase insulin secretion during the GTT. LOKO mice had reduced fasting insulin at the start of the GTT and were unable to appropriately increase plasma insulin after exogenous glucose administration. In fact, they exhibited an inappropriate drop in insulin levels at thirty minutes into the GTT, a time at which

compensatory insulin production should be peaking. Glucose intolerance in the face of insulinopenia strongly suggests that loss of LXRs impairs pancreatic function in LOKO mice.

LOKO mice are profoundly sensitive to exogenous insulin

To quantify peripheral insulin sensitivity and discriminate the effects of LXR deletion on muscle and liver insulin action under matched insulin exposure, we performed hyperinsulinemiceuglycemic clamp studies. Animal weights and basal glucose turnover rates were not significantly different between OB and LOKO mice (n=15 and 8, respectively; Fig. 3D). The glucose infusion rate required to maintain euglycemia (a measure of whole body insulin sensitivity) was approximately twice as high in LOKO compared to OB mice (27 ± 2.5 mg/kg/min vs. 13 ± 1.4 mg/kg/min, P = 0.0001; Fig. 3D). LOKO mice also showed a marked improvement in insulin-stimulated suppression of hepatic glucose production (HGP). In addition, the insulin-stimulated glucose disposal rate (IS-GDR) into peripheral tissues (primarily muscle) was nearly doubled in LOKO mice (15 ± 1.6 mg/kg/min vs. 8 ± 1.6 mg/kg/min, P = 0.0113), indicative of markedly improved peripheral insulin sensitivity. Improved insulin signaling was confirmed in livers from LOKO mice, as phospho-Akt was substantially increased under the glucose clamp conditions (Fig. 3E). Collectively, these findings show that LXR deletion in OB mice ameliorates hepatic and peripheral insulin resistance. Furthermore, the endogenous pancreatic defect appears to be the primary reason for glucose intolerance in LOKO mice, since they have improved peripheral glucose disposal when insulin levels are not limiting.

To characterize the pancreatic defect in more detail, we isolated pancreata from both lean and obese animals and performed morphometric analysis of beta-cell mass and number. Lean mice (WT or DKO) have relatively few insulin-positive endocrine islets scattered evenly throughout the pancreas (Fig. S3A). We saw expansion of beta-cell mass in response to obesity in both OB and LOKO mice (as expected), but the total beta-cell mass and absolute number of beta-cells were substantially lower in LOKO mice (Fig. 3F and S3A). Interestingly, this finding correlated with markedly reduced numbers of proliferating beta-cells in LOKO mice as revealed by Ki-67 immunostaining (Fig. 3F). Apoptotic staining revealed very few TUNEL-positive cells in either genotype, and no overall differences (data not shown). Due to the difficulty in generating LOKO animals, we were unable to examine apoptosis in younger mice and therefore cannot exclude the possibility that increased beta-cell death may be a contributor to the reduced numbers observed in LOKO islets. Expression of LXR target genes in isolated islets (*Srebp-1c*, *Abca1*, *Fas*) was diminished, while insulin itself (*Ins*), the beta-cell glucose transporter (*Glut2*), and a marker of beta-cell development (*Nkx2.2*) were unchanged (Fig. S3B). Previous work in pancreatic cell lines has suggested that LXRβ might play a role in insulin secretion from beta-cells (Efanov et al., 2004; Zitzer et al., 2006). We confirmed that in isolated pancreatic islets, only LXRβ is expressed and functional (Fig. S3C). To address the contribution of pancreatic LXR expression to the LOKO phenotype, we performed real-time insulin secretion studies (“perifusion” studies) on islets isolated from OB mice with and without LXRβ. Surprisingly, insulin secretion in response to glucose was not affected by the loss of LXRβ expression (Fig. 3G), suggesting that LXR does not play an essential role in insulin secretion *per se*, and that the relative

insulinopenia of LOKO compared to OB mice is likely a result of decreased proliferation and/or survival of LXR-deficient beta-cells in the setting of obesity.

De novo lipogenesis is shifted from liver to adipose tissue in LOKO mice

Recent work showed that inactivation of the SREBP pathway in liver does not improve insulin sensitivity despite reducing steatosis (Moon et al., 2012). In line with these results, supplementing the diet of OB animals with the synthetic LXR ligand, GW3965, for either two or four weeks significantly improved the glucose tolerance profiles of OB mice, and these beneficial effects occurred despite worsening hepatic lipogenesis (Fig. S3D,E). Thus, reduction of hepatic steatosis alone was unlikely to account for the improved systemic insulin sensitivity in LOKO mice. We therefore hypothesized that improved insulin sensitivity in another tissue might be the primary basis for the metabolic improvement. Since LOKO mice have increased adipose mass (Fig. 1C), this prompted us to interrogate adipose tissue metabolism more closely.

LOKO mice exhibited visibly larger fat pads, consistent with increased triglyceride storage in this tissue (Figs. 1C and 4A). The number and size of adipocytes was not obviously different between the genotypes (Fig. 4A and data not shown). The increased fat pad mass in LOKO mice was unexpected given the reduction in hepatic lipogenesis and the fact that SREBP-1c expression is responsive to LXR agonist treatment in adipose as well as liver. To clarify the basis for the adipose phenotype, we performed transcriptional profiling on adipose tissue. As expected, the expression several adipose LXR target genes, such as *ApoD* (Hummasti et al., 2004), was reduced in LOKO mice (Fig. 4B). Remarkably, and in contrast to our observations in liver, the expression of genes important for lipogenesis (*Srebp1c, Scd1, Scd2, Acaca, Fasn, Dgat1, Dgat2)* and lipid uptake (*Pltp, Vldlr, Ldlr, Ldrap1, Lpl*,) were increased in LOKO fat depots. These results were validated in an expanded cohort of mice by real-time PCR (Fig. 4C and data not shown). This difference in adipose lipogenic gene expression was not observed between WT and LXR DKO mice, consistent with prior studies in lean animals (Kalaany et al., 2005).

Surprisingly, LOKO mice also showed clear evidence of enhanced PPARγ activity, a pathway that is known to be a powerful promoter of insulin sensitivity in OB mice. The expression of PPARγ itself and multiple PPARγ target genes (e.g. *aP2, Adrp, Adiponectin, Olr1, Cd36, Gpihbp1*) was increased in LOKO adipose tissue (Fig. 4B,C). This effect was tissue-specific, as expression levels of PPARγ were unchanged and its target gene aP2, were diminished in LOKO livers (data not shown). This was only observed on the OB background and was not apparent when comparing WT and LXR DKO mice on a B6 background (Fig. 4B). Consistent with the known beneficial effects of the adipose PPARγ pathway on systemic glucose homeostasis, the expression of genes related to insulin sensitivity and glucose homeostasis (*Insr, Irs1, Irs2, Irs3, Foxo1, Glut4, Fatp1*) was increased in LOKO fat (Fig. 4B,C). Analysis of glucose uptake in fat explants confirmed specific, increased glucose uptake into adipose tissue of LOKO mice compared to OB controls (Fig. 4D). The expression of genes involved in triglyceride mobilization (*Hsl, Atgl*) and those encoding lipid droplet associated-proteins (*Adrp, Tip-47, S3-12, Lsdp5*) were also

higher in LOKO mice (Fig. S4B). This observation is also consistent with activation of the PPARγ pathway, as all of these are PPAR targets.

Recent work has highlighted an important role for ChREBP-*β* in adipose lipogenesis and insulin sensitivity (Herman et al., 2012). Surprisingly, the expression of *Chrebp-β* was markedly increased in adipose tissue from LOKO mice compared to OB controls (Fig. 4E). The expression of *Chrebp-α* and its targets *Rgs-16* and *Txnip* was also elevated, albeit to a lesser degree (Fig. 4E). By contrast *Chrebp-β* and *Rgs-16* levels were decreased in livers of LOKO mice (Fig S4A), consistent with prior work showing that *Chrebp* is an LXR target gene in liver (Cha and Repa, 2007). Together with the recent study of Herman et al. (Herman et al., 2012), these data strongly suggest that increased activity of ChREBP-β contributes to the enhanced adipose tissue lipogenic activity and insulin sensitivity of LOKO mice. Thus, loss of LXR expression leads to increased activity of two major lipogenic transcription factor pathways, PPARγ and ChREBP-β, selectively in adipose tissue.

Since inflammation has been postulated to play an important role in adipose tissue insulin resistance, we examined the expression of macrophage markers in LOKO mice. Although staining for F4/80-positive macrophages did not show obvious differences between OB and LOKO mice by histology, more sensitive analysis of macrophage-associated genes suggested increased macrophage content and activity. There were increased levels of mRNA encoding macrophage surface proteins (CD68) and cytokines characteristic of both classically (M1) and alternatively (M2) activated macrophages, including *Ccl2*, *Tnf*α, *Arg1*, *Il-6*, *iNos*, and *Cd274* in adipose tissue from LOKO compared to OB mice (Fig. 4B,F). Histologically, the composition of the adipose tissue was similar between LOKO and OB mice (Fig. 4A). There were also increased levels of circulating inflammatory mediators in LOKO mice (Fig. S4C). Thus, the improved adipose insulin sensitivity in LOKO mice did not correlate with reduced macrophage infiltration or reduced inflammatory profiles. This observation suggests that increased macrophage content is not a dominant determinant of adipose insulin sensitivity in all contexts and that increased adipose lipid storage is beneficial, even in the setting of increased inflammation.

We also examined the ability of insulin to regulate gene expression in adipose tissue. Adipose *Srebp-1c* and *Fasn* expression were refractory to insulin in OB mice (Fig. 4G), presumably reflecting adipose tissue insulin resistance (Diraison et al., 2002; Grefhorst et al., 2005; Kim et al., 1998). *Glut4* expression is also reduced in obese (OB) adipose tissue (Fig. 4G) (Grefhorst et al., 2005). Remarkably, the induction of *Srebp-1c*, *Fasn*, *Glut4* and *Chrebp*-β by insulin was enhanced in LOKO mice, providing further evidence of improved adipose tissue insulin sensitivity (Fig. 4G). Collectively, these data suggest that PPARγ and ChREBP-β pathway activation is a primary cause of improved systemic insulin sensitivity in LOKO mice. Our data also show that the LXR pathway is dispensable for adipose SREBP-1c expression and lipogenesis in obesity, and that the absence of LXRs enhances the lipogenic response to insulin in OB mice. These findings corroborate prior data showing that the LXR pathway does not play a substantial role in promoting PPARγ expression or adipose tissue mass (Hummasti et al., 2004), as both of these parameters are increased in the genetic absence of LXRs.

Discussion

Although previous work has implicated LXRs in glucose homeostasis, diabetes, and insulin secretion (Efanov et al., 2004; Gerin et al., 2005; Laffitte et al., 2003; Mitro et al., 2007), no study has directly addressed the role of LXRs in obesity-related diabetes. In part, this is because LXR null mice lose adipose tissue mass with age and are resistant to obesity. Kalaany et al showed that LXRa null mice are resistant to obesity if cholesterol is present in the diet (Kalaany et al., 2005) and LXR DKO mice are refractory to obesity when fed a high fat diet (our unpublished results). We have shown here that global LXR deletion does not protect against genetic obesity, but has dramatic effects on insulin sensitivity, pancreatic beta-cell mass, and glucose homeostasis. Since both *Srebp1c* and *Scd1* are direct LXR target genes, one might have expected LOKO mice to phenocopy OB mice lacking these genes (Chu et al., 2006; Cohen et al., 2002; Moon et al., 2012; Repa et al., 2000a). However, in striking contrast to those models, loss of LXRs in the setting of obesity shifts the program of *de novo* lipogenesis from liver to fat, resulting in improved insulin sensitivity. This phenotype mimics the effect of PPARγ agonist administration and can be traced to the induction of the adipose PPARγ pathway. Collectively, our data suggest that sterol sensing by LXRs in obese states plays an important role in lipid and glucose homeostasis and key aspects of the metabolic syndrome.

We find that both hepatic lipid accumulation and insulin resistance are strongly influenced by LXR expression in the setting of obesity. Many studies have shown that hepatic lipid accumulation correlates with both inflammation and insulin resistance (Adams et al., 2005; Angulo and Lindor, 2001; Bard-Chapeau et al., 2005; Chiang et al., 2009; Erion et al., 2009; Gutierrez-Juarez et al., 2006; Jiang et al., 2005; Marchesini et al., 1999; Savage et al., 2007; Schenk et al., 2008; Shoelson et al., 2007; Yki-Jarvinen, 2005). LOKO livers have reduced triglyceride accumulation (steatosis) and inflammation, and show improved insulin sensitivity, consistent with the idea that hepatic lipid accumulation may be a causal factor. But the relationship between steatosis and insulin sensitivity is controversial and context-dependent, with several lines of evidence arguing against a causal link. First, liver-specific DGAT transgenic mice, in which the liver is overloaded with triglycerides, do not show insulin resistance (Monetti et al., 2007). Second, blocking VLDL secretion from the liver does not alter insulin sensitivity or peripheral lipid storage (Minehira et al., 2008). Finally, it was recently demonstrated that OB mice with liver-specific SCAP deficiency, in which all nuclear forms of Srebp-1c, -1a, and -2 are eliminated, are protected from hepatic steatosis, but remain insulin resistant (Moon et al., 2012). This latter result stands in stark contrast to our findings, and suggests that LXR signaling exerts effects on glucose homeostasis independent of its activation of SREBP-1c and its target genes in liver. It seems unlikely that triglycerides and fatty-acyl lipids can be the sole determinants of hepatic insulin sensitivity or that loss of hepatic SREBP-1c activity alone can account for the metabolic phenotype of LOKO mice. Other types of hepatic lipids may also impact insulin signaling (Scapa et al., 2008), some of which may be under the control of LXRs. Also, we have not excluded the possibility of a LXR-controlled hepatic non-lipid signaling molecule (e.g. hormone or other peptide) that mediates systemic insulin resistance. However, our data are most consistent

with the conclusion that reduced hepatic triglyceride levels in liver cannot alone explain improved insulin sensitivity in LOKO mice.

Our data point to improved adipose tissue lipid storage and PPARγ pathway activation as the central mediator of improved insulin sensitivity in LOKO mice. We have uncovered a previously unrecognized connection between LXR signaling and the adipose PPARγ and ChREBP-β pathways in the setting of obesity. Activation of PPARγ in fat by thiazolidinedione ligands promotes adipose lipid storage and secondarily increases insulin sensitivity in liver and muscle (Tontonoz and Spiegelman, 2008). Recently, a novel isoform of ChREBP in adipose tissue has been shown to regulate glucose metabolism and track with insulin sensitivity (Herman et al., 2012). The ChREBP-β pathway is induced by GLUT4, itself a target of both PPAR (Tontonoz and Spiegelman, 2008) and LXR (Laffitte et al., 2003). While hepatic *de novo* lipogenesis is lost in LOKOs, there is a reciprocal increase of the same program in adipose tissue, with a concomitant up-regulation of PPARγ, ChREBP-β and their downstream targets. With respect to insulin sensitivity, the LOKO phenotype mimics the effect of PPARγ agonist administration and is consistent with the proposed beneficial effects of adipose lipogenesis. Our data show that adipose lipogenic gene expression, lipid storage and adipogenesis are not dependent on LXR expression as has been previously suggested (Juvet et al., 2003; Seo et al., 2004). Moreover, we show that loss of adipose LXR signaling actually leads to compensatory upregulation of both the PPARγ and ChREBP-β in obese but not lean mice. We have therefore established that LXRs act as physiologic suppressors of the PPARγ and ChREBP-β pathways, specifically in the obese state.

The ability of LXRs to regulate inflammation might also have been expected to impact the metabolic phenotype of OB mice (Zelcer and Tontonoz, 2006). Inflammatory signaling is postulated to be an important determinant of insulin sensitivity, with increased inflammation associated with insulin resistance (Arkan et al., 2005; Cai et al., 2005; Saberi et al., 2009). LXRs are negative regulators of inflammation in several cell types, including macrophages (Joseph et al., 2003; Tontonoz and Mangelsdorf, 2003) and non-parenchymal cells of the liver (Beaven et al., 2011). We previously reported that loss of bone marrow LXRα and LXRβ expression did not alter insulin resistance in high fat diet-fed mice (Marathe et al., 2009). In the present study, we show that loss of LXRs de-repressed inflammatory marker expression in obese adipose tissue and increased macrophage content, but the tissue was still more insulin sensitive. It is important to consider whole body insulin sensitivity in LOKO mice in light of both adipose-intrinsic and -extrinsic factors. In LOKO fat, the increased PPARγ signaling—a hallmark of improved insulin sensitivity—exists despite a pro-inflammatory state in this tissue. But multiple, extrinsic improvements in liver (i.e. steatosis, inflammation, and insulin sensitivity) are also potential contributors to whole body insulin sensitivity. The reciprocal changes in hepatic and adipose inflammatory markers would appear to negate each other in this model of obesity, suggesting that changes in metabolism, rather than inflammation, play the dominant role in determining insulin sensitivity, at least in this context. We anticipate that liver and adipose specific knockouts for LXRs will be invaluable for further delineating the metabolic dialogue between hepatic steatosis and visceral adiposity.

A surprising and apparently paradoxical finding of this study is that LOKO mice are glucose intolerant despite being more insulin sensitive. The explanation for glucose intolerance in LOKO mice is a pancreatic defect relating to total insulin quantity, as beta-cell numbers and mass are reduced in LOKO mice (Figs. 3F and S3A). Improved insulin sensitivity in LOKO mice is offset by a relative lack of insulin availability for their severe degree of obesity (Fig. 3A-C). Despite having glycosuria, there is no evidence that urinary glucose loss has a major impact on energy homeostasis in LOKO mice, since they have identical body weights (Fig. 1A) and energy expenditure (Fig. S1) when compared to OB mice. Other investigators have reported the presence of increased urinary output in older (>12 months) LXRβ deficient mice (Gabbi et al., 2012), and we also find that LOKO mice have polydipsia—a hallmark finding of diabetes (Fig. S1B). Previous papers have reported that loss of LXR signaling compromises glucose-stimulated insulin secretion (Chuang et al., 2008; Efanov et al., 2004; Gerin et al., 2005; Zitzer et al., 2006). We therefore extended our studies to examine freshly isolated LXR-deficient pancreatic islets exposed to both low or high glucose and did not find a defect in their ability to secrete insulin (Fig. 3G). Instead, reduced beta-cell mass (and therefore total beta-cell number) was linked to decreased proliferation of beta-cells (Figs. 3F and S3A). This data provides *in vivo* evidence that LXRs have an important role in post-natal beta-cell expansion in the setting of obesity.

Previously, it has been shown that LXR ligand activation improves glucose disposal (Cao et al., 2003; Dalen et al., 2003; Laffitte et al., 2003), but LXR agonists induce hypertriglyceridemia and hepatic steatosis by stimulating *de novo* lipogenesis in the liver, and therefore first generation LXR agonists are not an attractive option for treating the metabolic syndrome (Beaven and Tontonoz, 2006). The observation that global deletion of LXRs improves muscle, hepatic and adipose tissue insulin sensitivity in obesity raises the question of whether an LXR antagonist might have therapeutic utility for metabolic syndrome. Given the beneficial effects of LXR activation on cholesterol homeostasis and atherosclerosis, this seems unlikely. But the question of how an LXR antagonist would affect metabolic homeostasis in obese mice will nevertheless be important to investigate. In conclusion, our results demonstrate that LXR signaling is pivotal in coordinating insulin sensitivity, fat storage and beta-cell function in obesity. The integrated response to a glucose challenge appears to involve complementary effects of the LXR isotypes in different tissues. Future work with tissue-selective deletions of LXRs should help further unravel these pathways.

METHODS

Reagents

Synthetic LXR ligand GW3965 was provided by T. Willson (GlaxoSmithKline, Research Triangle Park, NC). For animal feeding experiments, GW3965 was compounded into standard mouse chow (0.012%) and fed to mice for 10 days (Research Diets D02061102CG, New Brunswick, NJ).

Animals

*Lxr*α−/− and *Lxr*β−/− mice on a C57/Bl6 background were originally provided by David Mangelsdorf (UT Southwestern Medical Center, Dallas). These animals were bred to *ob/+* heterozygotes purchased from the Jackson Labs and backcrossed for at least ten generations in our facilities at UCLA. All animals were housed in a temperature-controlled room under a 12-hour light / 12-hour dark cycle under pathogen-free conditions. Mice had *ad lib* access to water and standard chow (Harlan NIH-31, 3.1 kcal/g, 23% calories from protein, 18% from fat, and 59% from carbohydrate). Animals in this study were harvested at 24 weeks of age or between 16-18 weeks for islet cell isolations. All animal experiments were approved by the Institutional Animal Care and Research Advisory Committee of the University of California, Los Angeles.

Indirect Calorimetry

Animals at 12, 16, or 20 weeks of age were housed individually in a series of eight airtight chambers designed to assess the metabolic activity across three light (12 hour) / dark (12 hour) cycles (Oxymax, Columbus Instruments, Columbus, OH). Animals were acclimated to the chambers over the first 48 hours and data were collected over the subsequent 24. The mice had free access to water and powdered food presented from a food hopper attached to a scale, with the amounts of food and water consumed recorded. The rate of oxygen consumption (V_{O2}) and carbon dioxide production (V_{CO2}) were calculated and averaged over the entire final 24 hour period as well as for the light and dark cycle for each mouse. The respiratory exchange ratio (an approximation of R_Q) is calculated from the ratio V_{CO2}/V_{O2}. Ambulatory activity was measures by interruption of dual-axis infrared beams. Data were analyzed by Oxymax software provided by the manufacturer (Columbus Instruments, OH).

Glucose Tolerance Tests

For glucose tolerance tests, mice were fasted for 6 hours prior to a single intraperitoneal injection of glucose (1 g / kg). Blood sugars were measured by a nick in a tail vein and analyzed on either a handheld glucometer (AccuChek, Roche Diagnostics) or HemoCue blood glucose analyzer (HemoCue, Sweden). For insulin determinations, a second sample was taken at each time point and serum immediately separated by centrifugation with the aliquot snap frozen. Insulin levels were determined by an ultrasensitive mouse insulin ELISA kit according to the manufacturer's instructions (Crystal Chem and Mercodia) or by multiplexed bead assay (Luminex, Millipore). In some experiments, mice were fed a diet containing GW3965 at (0.012%) for 10 days. No difference in food consumption was seen between animals fed the ligand-containing diet or the reference diet.

Hyperinsulinemic – Euglycemic Clamps

Clamp studies to assess skeletal muscle and hepatic insulin sensitivity were performed following a six hour fast on chronically cannulated (dual jugular cannulae) mice as previously described (Hevener et al., 2003; Hevener et al., 2007). The glucose turnover rate was calculated at basal and at steady state during hyperinsulinemia. Briefly, at –90 min, a primed constant infusion of [3-^{3}H] D-glucose (Perkin Elmer NET331; 5 μCi/h) was

initiated. At time 0 min, a basal blood sample was drawn from the tail for the determination of glucose specific activity. Following basal sampling, dextrose (50%) and insulin (25 $mU•kg^{-1}•min^{-1}$, Novolin, Novo Nordisk) plus tracer (5 μCi/h) infusions were initiated simultaneously, and glucose levels clamped at euglycemia using a variable glucose infusion rate (GIR). Rates of glucose appearance and disappearance were calculated using the Steele equation for steady state glucose kinetics (Steele et al., 1959). Skeletal muscle and liver insulin sensitivity are reflected by the insulin-stimulated glucose disposal rate (IS-GDR) and the insulin-stimulated percent suppression of hepatic glucose production (HGP) respectively. Differences in IS-DGR and HGP were detected by ANOVA, with significance set a priori at $P < 0.05$.

Tissue, serum, and histologic analysis

Animals were fasted for 6 hours prior to sacrifice and blood collected by direct cardiac puncture with serum separated by centrifugation at 8000 rpm for 5 minutes at 4°C. Alanine and aspartate aminotransferases were determined by standard colorimetric analysis at our core facilities (UCLA Department of Laboratory and Animal Medicine). At the time of harvest, a small piece of liver was snap frozen in liquid nitrogen for future RNA extraction. The largest lobe of the liver was preserved for 24-48 hours in 10% formalin (w/v) and then transferred to 50% ethanol and kept at 4°C until taken for sectioning and staining with haematoxylin and eosin by the UCLA Translational Pathology Core Laboratory. The left epididymal WAT pad was weighed and frozen as well as the leg muscle groups. The pancreas was dissected out, trimmed of all connective tissue, and weighed. The entire pancreas was fixed in 10% formalin (w/v) and then transferred to 50% ethanol 24-48 hours later for sectioning and staining. Urine was analyzed for glycosuria using rapid (30 second) reagent strips (Bayer). Plasma lipids were fractionated using an FPLC system as previously described (Hedrick et al., 1993) and quantified by area under the curve. NEFA levels were measured by a colorimetric enzymatic assay (Wako) with standards prepared from 1 mM oleic acid. Optical density was measured at 550 nm. Microscopic sections were viewed on a Zeiss Axioskop 2 and images captured with a Zeiss CCD camera using AxioVision software (Zeiss). For 2-deoxyglucose (2-DG) uptake into isolated adipose tissue pieces (~0.3 cc) were sampled from perigonadal fat and placed in Krebs Henseleit Buffer containing 0.1% BSA, 1 mM sodium pyruvate, 1 mM mannitol and 1 mM 2-deoxy glucose. ^{3}H-2-deoxy glucose (3 μCi/ml) and ^{14}C-mannitol (0.053 μCi/ml) were to the incubation media for 30 min. Tissue was homogenized and glucose uptake specificity was determined by comparison to mannitol uptake.

Pancreatic Islet Morphology, Isolation, and Perifusion Studies

Pancreata removed at the time of sacrifice were embedded in paraffin and longitudinally sectioned (4 μM) through the head, body, and tail through the maximal width. Sections were stained for haematoxylin / eosin, insulin (guinea pig anti-insulin, 1:100; Zymed, Carlsbad, CA) as previously described (Janson et al., 1996). The beta-cell mass was measured by first quantifying pancreatic cross-sectional area positive for insulin and multiplying this by the pancreatic weight.

Primary islets were isolated from *ob/ob* mice as previously described (Huang et al., 2007). Briefly, mice were euthanized with isoflurane and the bile duct clamped at the entrance to the duodenum. The pancreatic duct was then cannulated and perfused with a solution containing HBSS (Invitrogen), 25 mM HEPES (Invitrogen), 0.23 mg/mL collagenase (Liberase, Roche) and 0.1 mg/mL DNAse (Roche). The pancreas was then surgically removed and placed in a glass vial containing ice-cold collagenase solution and digested for 20 minutes at 37°C and dispersed by gentle agitation for 30 seconds. After washing the islets are separated from the debris by differential density centrifugation over Histopaque (Sigma). The islets migrate at the medium / Histopaque interface, which is collected, washed, and islets handpicked under the microscope.

For specific insulin secretion assays, mouse islets were isolated by the method described above and recovered overnight in RPMI culture medium supplemented in 11 mmol/L glucose and 10% fetal bovine serum at 37°C in humidified air containing 5% CO_2. Islet perifusion experiments were performed using a previously validated perifusion system (ACUSYST-S, Cellex Biosciences, Inc., Minneapolis, MN) for measurements of insulin secretion. Isolated islets were first exposed to 40 minutes of basal glucose perfusate (4mM glucose in Krebs Ringer bicarbonate buffer supplemented with 0.2% serum albumin, preheated to 37°C, and oxygenated with 95% O_2 and 5% CO_2) followed by 40 minutes of hyperglycemic perfusate (16 mM glucose). Each perifusion chamber contained 20 islets, and the effluent was collected in 4-min intervals for subsequent determination of insulin concentrations by standard mouse insulin ELISA assay (Mercodia) (Song et al., 2002).

RNA and Protein Analysis

RNA from tissue or isolated islets was extracted using TRIzol (Invitrogen) according to the manufacturer's directions. One microgram of total RNA was reverse transcribed using iScript cDNA Synthesis Kit (Biorad). Sybergreen (Diagenode) real-time quantitative PCR assays were performed using an Applied Biosystems 7900HT sequence detector. Results are the means of duplicate experiments (pancreatic islet cells) or the means of harvested groups of mice, normalized to 36B4. Specific primer sequences are available upon request. For Western blotting, liver homogenates were prepared with RIPA lysis buffer containing protease inhibitors (Complete Mini, Roche), PMSF, NaF, and sodium orthovanadate. 25 μg protein was separated by SDS-PAGE and transferred to PVDF membranes. These were then probed with anti-Akt, anti-phosho-Akt, or anti-tubulin antibodies (Cell Signaling). After HRP-tagged secondary antibody incubation, chemiluminescence (ECL Plus, GE) was used to detect protein bands. Band density was quantified using ImageJ.

Statistical Analysis

Statistics were performed using Student's t test (2 groups), or ANOVA (> 2 groups) with post-tests to compare to the control group. Data are presented as means ± SEM and taken as statistically significant at $P < 0.05$.

Supplementary Material

Refer to Web version on PubMed Central for supplementary material.

Acknowledgments

We thank David Mangelsdorf for the original LXR null mice, and Tim Willson for GW3965. We also thank Larry Castellani for his assistance in with FPLC and Tom Vallim and Elizabeth Tarling for assistance with hepatic lipid quantifications. We thank Jon Salazar for his assistance in maintaining the mouse colonies. P.T. is an Investigator of the Howard Hughes Medical Institute. This work was supported by NIH Training Grant T32KD07180-30, UCLA Center for Ulcer Research and Education (CURE) Pilot and Feasibility Study Grant 441349-BB-39108, and a generous gift from Brad and Joan Jones (to S.W.B.) and grants HL66088 and HL30568 (to P.T.) and DRC grant P30 DK063491.

Abbreviations

LXR	Liver X receptor
LOKO	*ob/ob Lxr*αβ−/−
DKO	*Lxr*αβ−/−
OB	ob/ob
WT	wild-type
GTT	glucose tolerance test
ITT	insulin tolerance test

References

Adams LA, Lymp JF, St Sauver J, Sanderson SO, Lindor KD, Feldstein A, Angulo P. The natural history of nonalcoholic fatty liver disease: a population-based cohort study. Gastroenterology. 2005; 129:113–121. [PubMed: 16012941]

Angulo P, Lindor KD. Treatment of nonalcoholic fatty liver: present and emerging therapies. Semin Liver Dis. 2001; 21:81–88. [PubMed: 11296699]

Arkan MC, Hevener AL, Greten FR, Maeda S, Li ZW, Long JM, Wynshaw-Boris A, Poli G, Olefsky J, Karin M. IKK-beta links inflammation to obesity-induced insulin resistance. Nat Med. 2005; 11:191–198. [PubMed: 15685170]

Bard-Chapeau EA, Hevener AL, Long S, Zhang EE, Olefsky JM, Feng GS. Deletion of Gab1 in the liver leads to enhanced glucose tolerance and improved hepatic insulin action. Nat Med. 2005; 11:567–571. [PubMed: 15821749]

Beaven SW, Tontonoz P. Nuclear receptors in lipid metabolism: targeting the heart of dyslipidemia. Annu Rev Med. 2006; 57:313–329. [PubMed: 16409152]

Beaven SW, Wroblewski K, Wang J, Hong C, Bensinger S, Tsukamoto H, Tontonoz P. Liver X receptor signaling is a determinant of stellate cell activation and susceptibility to fibrotic liver disease. Gastroenterology. 2011; 140:1052–1062. [PubMed: 21134374]

Bensinger SJ, Bradley MN, Joseph SB, Zelcer N, Janssen EM, Hausner MA, Shih R, Parks JS, Edwards PA, Jamieson BD, et al. LXR signaling couples sterol metabolism to proliferation in the acquired immune response. Cell. 2008; 134:97–111. [PubMed: 18614014]

Bradley MN, Hong C, Chen M, Joseph SB, Wilpitz DC, Wang X, Lusis AJ, Collins A, Hseuh WA, Collins JL, et al. Ligand activation of LXR beta reverses atherosclerosis and cellular cholesterol overload in mice lacking LXR alpha and apoE. J Clin Invest. 2007; 117:2337–2346. [PubMed: 17657314]

Cai D, Yuan M, Frantz DF, Melendez PA, Hansen L, Lee J, Shoelson SE. Local and systemic insulin resistance resulting from hepatic activation of IKK-beta and NF-kappaB. Nat Med. 2005; 11:183–190. [PubMed: 15685173]

Cao G, Liang Y, Broderick CL, Oldham BA, Beyer TP, Schmidt RJ, Zhang Y, Stayrook KR, Suen C, Otto KA, et al. Antidiabetic action of a liver x receptor agonist mediated by inhibition of hepatic gluconeogenesis. J Biol Chem. 2003; 278:1131–1136. [PubMed: 12414791]

Cha JY, Repa JJ. The liver X receptor (LXR) and hepatic lipogenesis. The carbohydrate-response element-binding protein is a target gene of LXR. J Biol Chem. 2007; 282:743–751. [PubMed: 17107947]

Chiang SH, Bazuine M, Lumeng CN, Geletka LM, Mowers J, White NM, Ma JT, Zhou J, Qi N, Westcott D, et al. The protein kinase IKKepsilon regulates energy balance in obese mice. Cell. 2009; 138:961–975. [PubMed: 19737522]

Chu K, Miyazaki M, Man WC, Ntambi JM. Stearoyl-coenzyme A desaturase 1 deficiency protects against hypertriglyceridemia and increases plasma high-density lipoprotein cholesterol induced by liver X receptor activation. Mol Cell Biol. 2006; 26:6786–6798. [PubMed: 16943421]

Chuang JC, Cha JY, Garmey JC, Mirmira RG, Repa JJ. Research resource: nuclear hormone receptor expression in the endocrine pancreas. Mol Endocrinol. 2008; 22:2353–2363. [PubMed: 18669644]

Cohen P, Miyazaki M, Socci ND, Hagge-Greenberg A, Liedtke W, Soukas AA, Sharma R, Hudgins LC, Ntambi JM, Friedman JM. Role for stearoyl-CoA desaturase-1 in leptin-mediated weight loss. Science. 2002; 297:240–243. [PubMed: 12114623]

Commerford SR, Vargas L, Dorfman SE, Mitro N, Rocheford EC, Mak PA, Li X, Kennedy P, Mullarkey TL, Saez E. Dissection of the insulin-sensitizing effect of liver X receptor ligands. Mol Endocrinol. 2007; 21:3002–3012. [PubMed: 17717069]

Cummins CL, Volle DH, Zhang Y, McDonald JG, Sion B, Lefrancois-Martinez AM, Caira F, Veyssiere G, Mangelsdorf DJ, Lobaccaro JM. Liver X receptors regulate adrenal cholesterol balance. J Clin Invest. 2006; 116:1902–1912. [PubMed: 16823488]

Dalen KT, Ulven SM, Bamberg K, Gustafsson JA, Nebb HI. Expression of the insulin-responsive glucose transporter GLUT4 in adipocytes is dependent on liver X receptor alpha. J Biol Chem. 2003; 278:48283–48291. [PubMed: 12970362]

Diraison F, Dusserre E, Vidal H, Sothier M, Beylot M. Increased hepatic lipogenesis but decreased expression of lipogenic gene in adipose tissue in human obesity. Am J Physiol Endocrinol Metab. 2002; 282:E46–51. [PubMed: 11739082]

Efanov AM, Sewing S, Bokvist K, Gromada J. Liver X receptor activation stimulates insulin secretion via modulation of glucose and lipid metabolism in pancreatic beta-cells. Diabetes 53 Suppl. 2004; 3:S75–78.

Erion DM, Ignatova ID, Yonemitsu S, Nagai Y, Chatterjee P, Weismann D, Hsiao JJ, Zhang D, Iwasaki T, Stark R, et al. Prevention of hepatic steatosis and hepatic insulin resistance by knockdown of cAMP response element-binding protein. Cell Metab. 2009; 10:499–506. [PubMed: 19945407]

Farese RV Jr. Zechner R, Newgard CB, Walther TC. The problem of establishing relationships between hepatic steatosis and hepatic insulin resistance. Cell Metab. 2012; 15:570–573. [PubMed: 22560209]

Gabbi C, Kong X, Suzuki H, Kim HJ, Gao M, Jia X, Ohnishi H, Ueta Y, Warner M, Guan Y, et al. Central diabetes insipidus associated with impaired renal aquaporin-1 expression in mice lacking liver X receptor beta. Proc Natl Acad Sci U S A. 2012; 109:3030–3034. [PubMed: 22323586]

Gerin I, Dolinsky VW, Shackman JG, Kennedy RT, Chiang SH, Burant CF, Steffensen KR, Gustafsson JA, MacDougald OA. LXRbeta is required for adipocyte growth, glucose homeostasis, and beta cell function. J Biol Chem. 2005; 280:23024–23031. [PubMed: 15831500]

Grefhorst A, Parks EJ. Reduced insulin-mediated inhibition of VLDL secretion upon pharmacological activation of the liver X receptor in mice. J Lipid Res. 2009; 50:1374–1383. [PubMed: 19287042]

Grefhorst A, van Dijk TH, Hammer A, van der Sluijs FH, Havinga R, Havekes LM, Romijn JA, Groot PH, Reijngoud DJ, Kuipers F. Differential effects of pharmacological liver X receptor activation on hepatic and peripheral insulin sensitivity in lean and ob/ob mice. Am J Physiol Endocrinol Metab. 2005; 289:E829–838. [PubMed: 15941783]

Gutierrez-Juarez R, Pocai A, Mulas C, Ono H, Bhanot S, Monia BP, Rossetti L. Critical role of stearoyl-CoA desaturase-1 (SCD1) in the onset of diet-induced hepatic insulin resistance. J Clin Invest. 2006; 116:1686–1695. [PubMed: 16741579]

Hedrick CC, Castellani LW, Warden CH, Puppione DL, Lusis AJ. Influence of mouse apolipoprotein A-II on plasma lipoproteins in transgenic mice. J Biol Chem. 1993; 268:20676–20682. [PubMed: 8376417]

Herman MA, Peroni OD, Villoria J, Schon MR, Abumrad NA, Bluher M, Klein S, Kahn BB. A novel ChREBP isoform in adipose tissue regulates systemic glucose metabolism. Nature. 2012; 484:333–338. [PubMed: 22466288]

Hevener AL, He W, Barak Y, Le J, Bandyopadhyay G, Olson P, Wilkes J, Evans RM, Olefsky J. Muscle-specific Pparg deletion causes insulin resistance. Nat Med. 2003; 9:1491–1497. [PubMed: 14625542]

Hevener AL, Olefsky JM, Reichart D, Nguyen MT, Bandyopadyhay G, Leung HY, Watt MJ, Benner C, Febbraio MA, Nguyen AK, et al. Macrophage PPAR gamma is required for normal skeletal muscle and hepatic insulin sensitivity and full antidiabetic effects of thiazolidinediones. J Clin Invest. 2007; 117:1658–1669. [PubMed: 17525798]

Hong C, Kidani Y, N AG, Phung T, Ito A, Rong X, Ericson K, Mikkola H, Beaven SW, Miller LS, et al. Coordinate regulation of neutrophil homeostasis by liver X receptors in mice. J Clin Invest. 2012; 122:337–347. [PubMed: 22156197]

Huang CJ, Haataja L, Gurlo T, Butler AE, Wu X, Soeller WC, Butler PC. Induction of endoplasmic reticulum stress-induced beta-cell apoptosis and accumulation of polyubiquitinated proteins by human islet amyloid polypeptide. Am J Physiol Endocrinol Metab. 2007; 293:E1656–1662. [PubMed: 17911343]

Hummasti S, Laffitte BA, Watson MA, Galardi C, Chao LC, Ramamurthy L, Moore JT, Tontonoz P. Liver X receptors are regulators of adipocyte gene expression but not differentiation: identification of apoD as a direct target. J Lipid Res. 2004; 45:616–625. [PubMed: 14703507]

Janson J, Soeller WC, Roche PC, Nelson RT, Torchia AJ, Kreutter DK, Butler PC. Spontaneous diabetes mellitus in transgenic mice expressing human islet amyloid polypeptide. Proc Natl Acad Sci U S A. 1996; 93:7283–7288. [PubMed: 8692984]

Jiang G, Li Z, Liu F, Ellsworth K, Dallas-Yang Q, Wu M, Ronan J, Esau C, Murphy C, Szalkowski D, et al. Prevention of obesity in mice by antisense oligonucleotide inhibitors of stearoyl-CoA desaturase-1. J Clin Invest. 2005; 115:1030–1038. [PubMed: 15761499]

Joseph SB, Bradley MN, Castrillo A, Bruhn KW, Mak PA, Pei L, Hogenesch J, O'Connell R M, Cheng G, Saez E, et al. LXR-dependent gene expression is important for macrophage survival and the innate immune response. Cell. 2004; 119:299–309. [PubMed: 15479645]

Joseph SB, Castrillo A, Laffitte BA, Mangelsdorf DJ, Tontonoz P. Reciprocal regulation of inflammation and lipid metabolism by liver X receptors. Nat Med. 2003; 9:213–219. [PubMed: 12524534]

Juvet LK, Andresen SM, Schuster GU, Dalen KT, Tobin KA, Hollung K, Haugen F, Jacinto S, Ulven SM, Bamberg K, et al. On the role of liver X receptors in lipid accumulation in adipocytes. Mol Endocrinol. 2003; 17:172–182. [PubMed: 12554745]

Kalaany NY, Gauthier KC, Zavacki AM, Mammen PP, Kitazume T, Peterson JA, Horton JD, Garry DJ, Bianco AC, Mangelsdorf DJ. LXRs regulate the balance between fat storage and oxidation. Cell Metab. 2005; 1:231–244. [PubMed: 16054068]

Kim JB, Sarraf P, Wright M, Yao KM, Mueller E, Solanes G, Lowell BB, Spiegelman BM. Nutritional and insulin regulation of fatty acid synthetase and leptin gene expression through ADD1/SREBP1. J Clin Invest. 1998; 101:1–9. [PubMed: 9421459]

Laffitte BA, Chao LC, Li J, Walczak R, Hummasti S, Joseph SB, Castrillo A, Wilpitz DC, Mangelsdorf DJ, Collins JL, et al. Activation of liver X receptor improves glucose tolerance through coordinate regulation of glucose metabolism in liver and adipose tissue. Proc Natl Acad Sci U S A. 2003; 100:5419–5424. [PubMed: 12697904]

Marathe C, Bradley MN, Hong C, Chao L, Wilpitz D, Salazar J, Tontonoz P. Preserved glucose tolerance in high-fat-fed C57BL/6 mice transplanted with PPARgamma−/−, PPARdelta−/−, PPARgammadelta−/−, or LXRalphabeta−/− bone marrow. J Lipid Res. 2009; 50:214–224. [PubMed: 18772483]

Marchesini G, Brizi M, Morselli-Labate AM, Bianchi G, Bugianesi E, McCullough AJ, Forlani G, Melchionda N. Association of nonalcoholic fatty liver disease with insulin resistance. Am J Med. 1999; 107:450–455. [PubMed: 10569299]

Minehira K, Young SG, Villanueva CJ, Yetukuri L, Oresic M, Hellerstein MK, Farese RV Jr. Horton JD, Preitner F, Thorens B, et al. Blocking VLDL secretion causes hepatic steatosis but does not

affect peripheral lipid stores or insulin sensitivity in mice. J Lipid Res. 2008; 49:2038–2044. [PubMed: 18515909]

Mitro N, Mak PA, Vargas L, Godio C, Hampton E, Molteni V, Kreusch A, Saez E. The nuclear receptor LXR is a glucose sensor. Nature. 2007; 445:219–223. [PubMed: 17187055]

Monetti M, Levin MC, Watt MJ, Sajan MP, Marmor S, Hubbard BK, Stevens RD, Bain JR, Newgard CB, Farese RV Sr. et al. Dissociation of hepatic steatosis and insulin resistance in mice overexpressing DGAT in the liver. Cell Metab. 2007; 6:69–78. [PubMed: 17618857]

Moon YA, Liang G, Xie X, Frank-Kamenetsky M, Fitzgerald K, Koteliansky V, Brown MS, Goldstein JL, Horton JD. The Scap/SREBP pathway is essential for developing diabetic fatty liver and carbohydrate-induced hypertriglyceridemia in animals. Cell Metab. 2012; 15:240–246. [PubMed: 22326225]

N AG, Bensinger SJ, Hong C, Beceiro S, Bradley MN, Zelcer N, Deniz J, Ramirez C, Diaz M, Gallardo G, et al. Apoptotic cells promote their own clearance and immune tolerance through activation of the nuclear receptor LXR. Immunity. 2009; 31:245–258. [PubMed: 19646905]

Olefsky JM, Glass CK. Macrophages, inflammation, and insulin resistance. Annu Rev Physiol. 2010; 72:219–246. [PubMed: 20148674]

Peet DJ, Turley SD, Ma W, Janowski BA, Lobaccaro JM, Hammer RE, Mangelsdorf DJ. Cholesterol and bile acid metabolism are impaired in mice lacking the nuclear oxysterol receptor LXR alpha. Cell. 1998; 93:693–704. [PubMed: 9630215]

Repa JJ, Liang G, Ou J, Bashmakov Y, Lobaccaro JM, Shimomura I, Shan B, Brown MS, Goldstein JL, Mangelsdorf DJ. Regulation of mouse sterol regulatory element-binding protein-1c gene (SREBP-1c) by oxysterol receptors, LXRalpha and LXRbeta. Genes Dev. 2000a; 14:2819–2830. [PubMed: 11090130]

Repa JJ, Turley SD, Lobaccaro JA, Medina J, Li L, Lustig K, Shan B, Heyman RA, Dietschy JM, Mangelsdorf DJ. Regulation of absorption and ABC1-mediated efflux of cholesterol by RXR heterodimers. Science. 2000b; 289:1524–1529. [PubMed: 10968783]

Ribas V, Drew BG, Le JA, Soleymani T, Daraei P, Sitz D, Mohammad L, Henstridge DC, Febbraio MA, Hewitt SC, Korach KS, Bensinger SJ, Hevener AL. Myeloid-specific estrogen receptor alpha deficiency impairs metabolic homeostasis and accelerates atherosclerotic lesion development. Proc Natl Acad Sci U S A. 2011; 108:16457–16462. [PubMed: 21900603]

Saberi M, Woods NB, de Luca C, Schenk S, Lu JC, Bandyopadhyay G, Verma IM, Olefsky JM. Hematopoietic cell-specific deletion of toll-like receptor 4 ameliorates hepatic and adipose tissue insulin resistance in high-fat-fed mice. Cell Metab. 2009; 10:419–429. [PubMed: 19883619]

Savage DB, Petersen KF, Shulman GI. Disordered lipid metabolism and the pathogenesis of insulin resistance. Physiol Rev. 2007; 87:507–520. [PubMed: 17429039]

Scapa EF, Pocai A, Wu MK, Gutierrez-Juarez R, Glenz L, Kanno K, Li H, Biddinger S, Jelicks LA, Rossetti L, et al. Regulation of energy substrate utilization and hepatic insulin sensitivity by phosphatidylcholine transfer protein/StarD2. Faseb J. 2008; 22:2579–2590. [PubMed: 18347010]

Schenk S, Saberi M, Olefsky JM. Insulin sensitivity: modulation by nutrients and inflammation. J Clin Invest. 2008; 118:2992–3002. [PubMed: 18769626]

Schultz JR, Tu H, Luk A, Repa JJ, Medina JC, Li L, Schwendner S, Wang S, Thoolen M, Mangelsdorf DJ, et al. Role of LXRs in control of lipogenesis. Genes Dev. 2000; 14:2831–2838. [PubMed: 11090131]

Seo JB, Moon HM, Kim WS, Lee YS, Jeong HW, Yoo EJ, Ham J, Kang H, Park MG, Steffensen KR, et al. Activated liver X receptors stimulate adipocyte differentiation through induction of peroxisome proliferator-activated receptor gamma expression. Mol Cell Biol. 2004; 24:3430–3444. [PubMed: 15060163]

Shoelson SE, Herrero L, Naaz A. Obesity, inflammation, and insulin resistance. Gastroenterology. 2007; 132:2169–2180. [PubMed: 17498510]

Song SH, Kjems L, Ritzel R, McIntyre SM, Johnson ML, Veldhuis JD, Butler PC. Pulsatile insulin secretion by human pancreatic islets. J Clin Endocrinol Metab. 2002; 87:213–221. [PubMed: 11788649]

Steele R, Altszuler N, Wall JS, Dunn A, De Bodo RC. Influence of adrenalectomy on glucose turnover and conversion to CO2: studies with C14 glucose in the dog. Am J Physiol. 1959; 196:221–230. [PubMed: 13627150]

Tontonoz P, Mangelsdorf DJ. Liver X receptor signaling pathways in cardiovascular disease. Mol Endocrinol. 2003; 17:985–993. [PubMed: 12690094]

Tontonoz P, Spiegelman BM. Fat and beyond: the diverse biology of PPARgamma. Annu Rev Biochem. 2008; 77:289–312. [PubMed: 18518822]

Yki-Jarvinen H. Fat in the liver and insulin resistance. Ann Med. 2005; 37:347–356. [PubMed: 16179270]

Zelcer N, Hong C, Boyadjian R, Tontonoz P. LXR regulates cholesterol uptake through Idol-dependent ubiquitination of the LDL receptor. Science. 2009; 325:100–104. [PubMed: 19520913]

Zelcer N, Tontonoz P. Liver X receptors as integrators of metabolic and inflammatory signaling. J Clin Invest. 2006; 116:607–614. [PubMed: 16511593]

Zitzer H, Wente W, Brenner MB, Sewing S, Buschard K, Gromada J, Efanov AM. Sterol regulatory element-binding protein 1 mediates liver X receptor-beta-induced increases in insulin secretion and insulin messenger ribonucleic acid levels. Endocrinology. 2006; 147:3898–3905. [PubMed: 16644917]

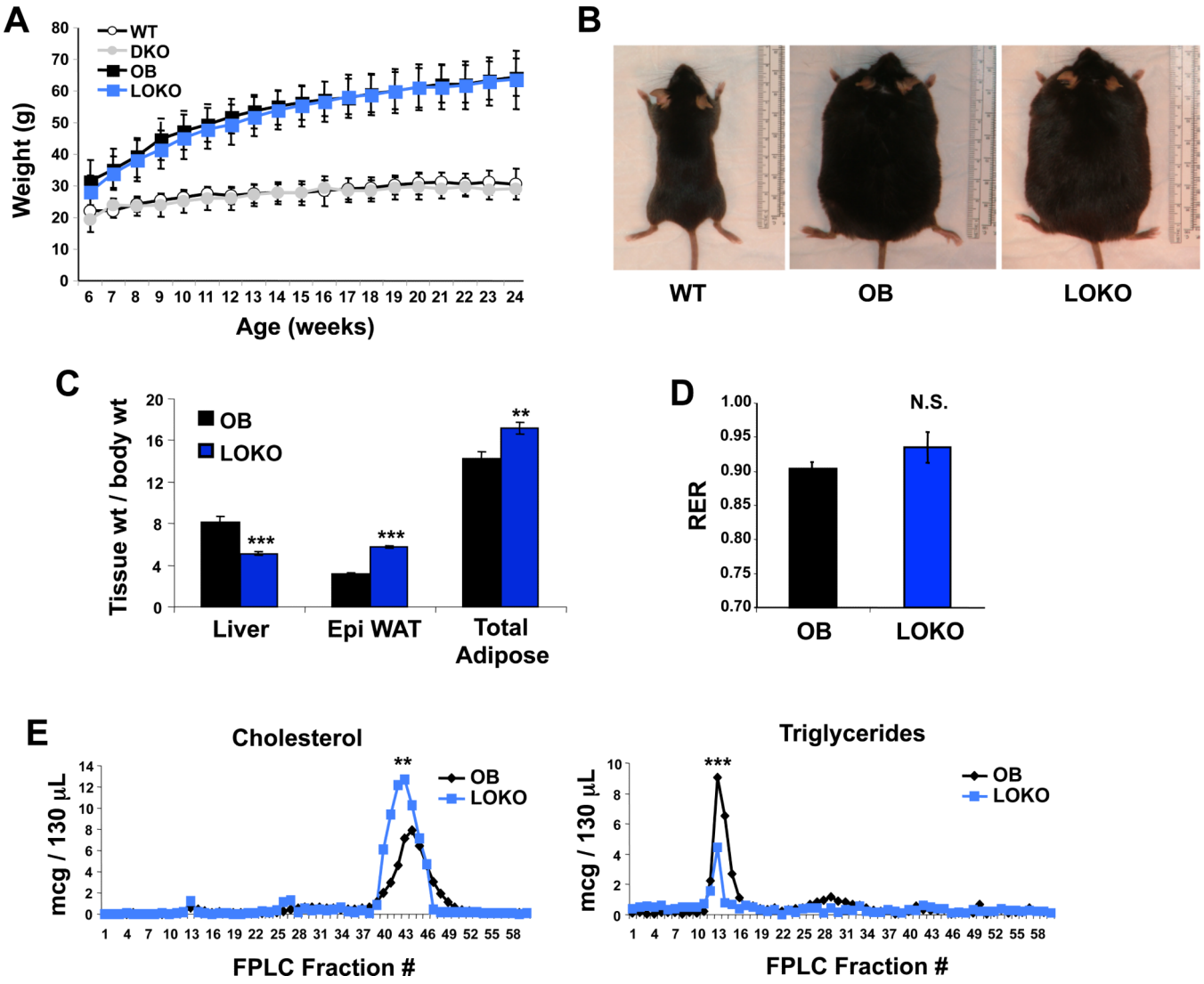

Figure 1. Characterization of LOKO mice

(A) Wild-type (WT), *Lxr*αβ−/− (DKO), *ob/ob* (OB), and *ob/ob Lxr*αβ−/− (LOKO) mice were weighed weekly. N = 10-11 WT or DKO, N = 20-33 OB or LOKO. No significant weight differences between OB and LOKO mice were observed. **(B)** Size comparison of lean (WT) and obese mice (OB and LOKO). **(C)** At 24 weeks of age, mice were fasted for 12 hours, euthanized, and organs harvested. Liver and WAT weight are shown normalized to total body weight (N = 19 OB, 17 LOKO). **(D)** Indirect calorimetry was performed on mice between 14 and 18 weeks of age. Mice were acclimatized to cages for 6+ hours and data then collected for an additional 72 hours (N = 7 OB, 8 LOKO). **(E)** Pooled plasma from OB and LOKO mice (N = 5-8) was analyzed by FPLC. Statistical analysis by 2-way ANOVA with Bonferroni post-tests (**A, E)** or Student's t-test (**C, D**): **, P < 0.01; ***, P < 0.001; N.S. not significant.

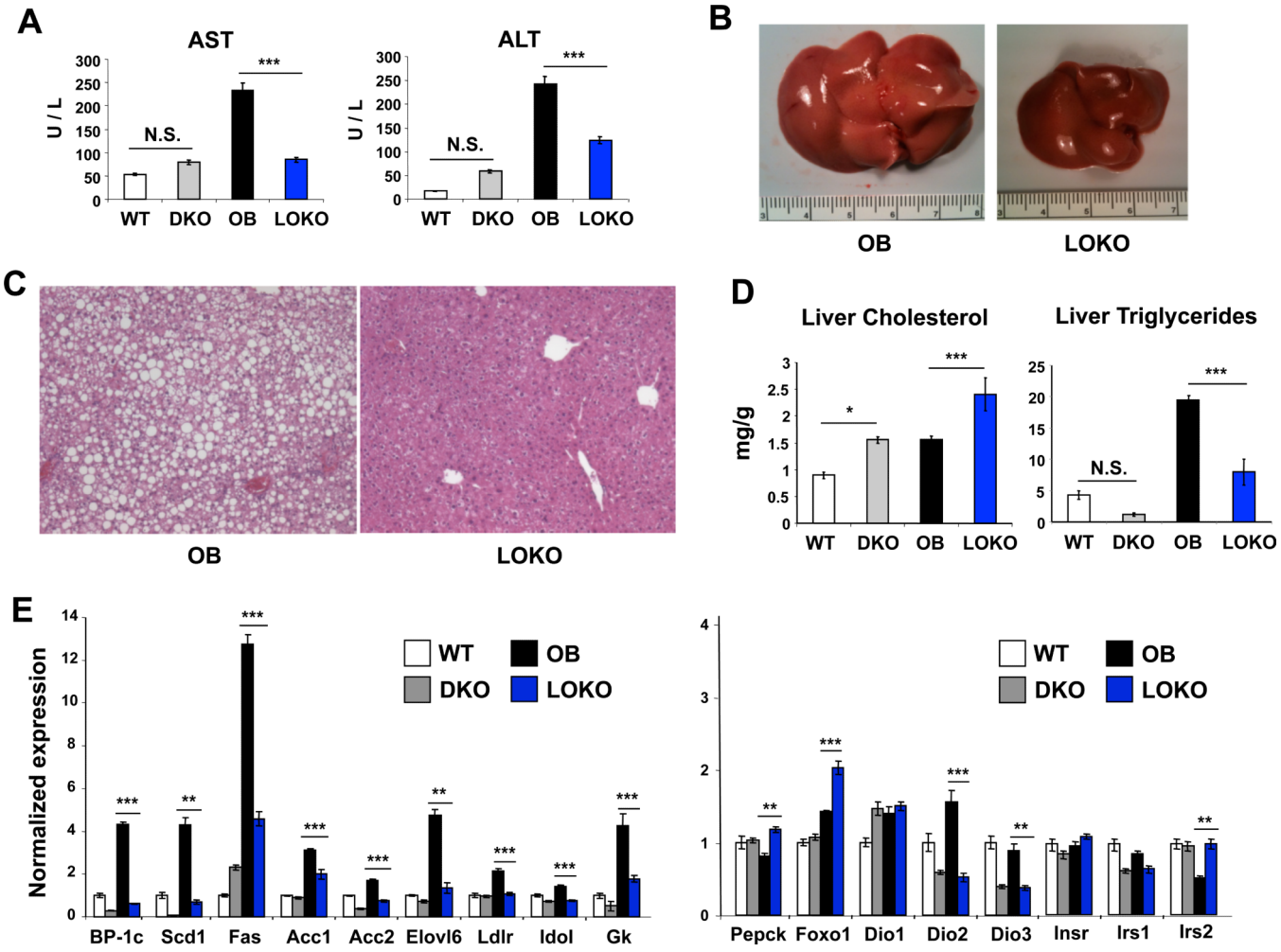

Figure 2. LOKO livers are rescued from hepatic steatosis

(A) Markers of hepatocellular necrosis (AST, ALT) were measured by colorimetric assay in WT, DKO, OB, and LOKO mice (N = 6-8 mice per group). **(B)** LOKO livers are smaller and lack significant steatosis by gross examination. **(C)** Representative H&E sections from OB and LOKO mice are shown. Magnification = 100×. **(D)** Hepatic lipids were extracted and quantified from WT, DKO, OB, and LOKO mice (N = 5-6 mice per group). **(E)** Hepatic gene expression was measured in WT, DKO, OB, and LOKO mice (N = 5-9 mice per group) at 24 weeks of age. Results are normalized first to expression of the housekeeping gene 36B4 and shown as fold induction over WT animals. Values are means +/− SEM. Statistical analysis by 1-way ANOVA with Bonferroni post-tests: *, $P < 0.05$; **, $P < 0.01$; ***, $P < 0.001$, N.S. not significant.

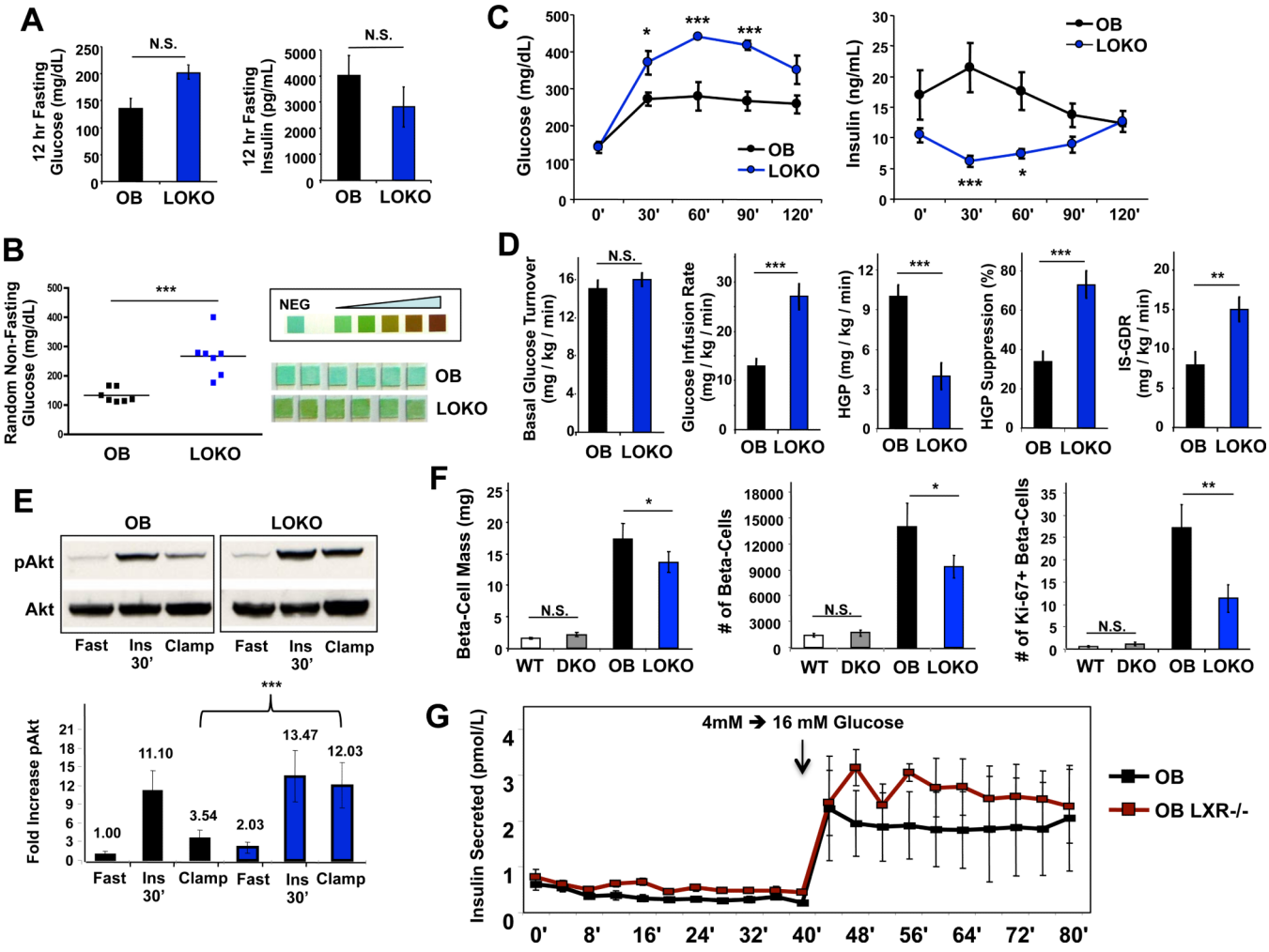

Figure 3. LOKO mice are glucose intolerant but insulin sensitive

(A) Borderline fasting hyperglycemia and insulinopenia in LOKO mice. Mice were fasted overnight and glucose measured by glucometer, and insulin, measured by multiplexed bead assay (Luminex, Millipore) (N=5 per group). **(B)** Random blood glucose levels from a separate group of OB and LOKO mice, showing significant hyperglycemia. Similar results were obtained in 3 separate experiments. Glycosuria in LOKO mice is shown by chemical reaction with clinical urine test strips. **(C)** Glucose tolerance tests were performed by I.P. injection of 1 mg/kg glucose into OB and LOKO mice (N=5 per group) fasted for 6 h. Time course measurements of blood glucose and insulin from the same experiment are shown. Values are means +/− SEM. This experiment was repeated 3 times in 2 different cohorts of mice. **(D)** LOKO mice are highly insulin sensitive in response to exogenous insulin. A separate cohort of OB (N = 15) and LOKO (N = 8) was analyzed by the hyperinsulinemic-euglycemic clamp technique as described in Methods. ISGDR, insulin-stimulated glucose disposal rate; HGP, hepatic glucose production. Values are expressed as means +/− SEM. **(E)** Western blotting for hepatic Akt, and its phosphorylated form (pSer473) showing increased basal pAkt expression in LOKO mice. Blotting was performed on whole livers from individual animals (n=3) of each genotype (OB, LOKO) under three conditions: i)

fasting for 6 hours [Fast], ii) fasting for 6 hours with a single intraperitoneal injection of insulin (12 U/kg) administered 30 minutes before sacrifice [Ins 30'], and iii) at the end of hyperinsulinemic-euglycemic clamps from Fig 3D [Clamp]. A single representative blot is shown. Band density was quantified by image analysis and expressed relative to the fasted OB animals. **(F)** Quantification of total beta-cell mass from pancreatic sections stained for insulin production (N = 10-15 mice per genotype). Additional sections were immunofluorescently stained for insulin and a proliferative marker, Ki-67, and hand counted for cell numbers (N = 10 -11 for each genotype; N = 277,990 individual beta-cells tabulated across all genotypes). The average number of beta-cells and proliferating (Ki-67+) beta-cells for each genotype are shown. **(G)** Pancreatic islets were isolated from obese mice as described in Methods for glucose-stimulated insulin perifusion studies. After overnight recovery, islets were exposed to a low basal level of glucose (4 mM) for 40 minutes and then switched into high glucose media (16 mM) for another 40 minutes. Samples of the perfusate were measured for islet-secreted insulin by ELISA (n=3 separate channels per time point). Statistical analysis by Student's t-test **(A, B, D, F)** or 2-way ANOVA with Bonferroni post-tests **(C, G)**: *, $P < 0.05$; **, $P < 0.01$; ***, $P < 0.001$.

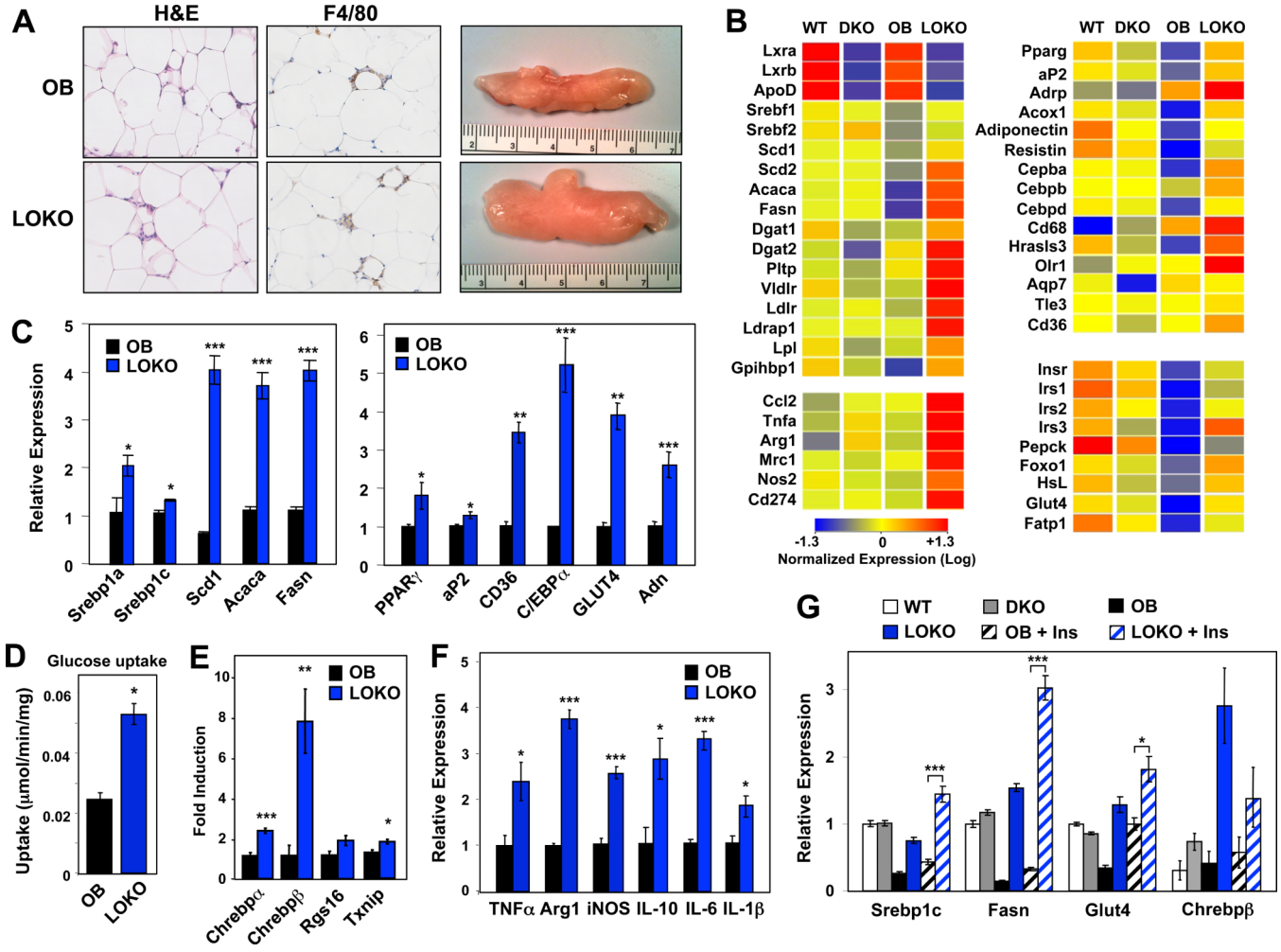

Figure 4. Activation of the adipose PPARγ pathway in LOKO mice

(A) H&E staining and gross morphology of epididymal fat pads from OB and LOKO mice. Magnification = 100×. **(B)** Exon gene array profiling (Affymetrix) was performed on pooled RNA from WT, DKO, OB, and LOKO mice (N = 5-8 mice per group). Global gene expression was filtered for genes showing at least a 2× change. Red demonstrates increased expression, while blue shows genes that are decreased. **(C)** Real-time quantitative gene expression validation from white adipose tissue. **(D)** Isotope-labeled glucose uptake in isolated fat pads from obese mice as described in Methods. **(E)** ChREBP pathway gene expression, **(F)** Inflammatory gene expression and **(G)** insulin-stimulated gene expression from white adipose tissue in lean, obese, and obese mice injected intraperitoneally with a single dose of insulin (12 U/kg) 30 minutes before sacrifice ('+ Ins'). Values are means +/− SEM. Statistical analysis by Student's t-test (**C-F)** or 1-way ANOVA **(G)** with Bonferroni post-tests: *, $P < 0.05$; **, $P < 0.01$; ***, $P < 0.001$.